

Energy Recuperation at the Hip Joint for Paraplegic Walking: Interaction Between Patient and Supportive Device

Conference Paper**Author(s):**

Auberger, Roland Adolf ; Riener, Robert; Russold, Michael F.; Dietl, Hans

Publication date:

2019

Permanent link:

<https://doi.org/10.3929/ethz-b-000366639>

Rights / license:

In Copyright - Non-Commercial Use Permitted

Originally published in:

<https://doi.org/10.1109/icorr.2019.8779491>

Energy Recuperation at the Hip Joint for Paraplegic Walking: Interaction Between Patient and Supportive Device

Roland Auberger, Robert Riener, Michael Friedrich Russold, Hans Dietl

Abstract— For patients with lower limb paralysis, wearable robotic systems are becoming increasingly important for regaining mobility. The actuation of these systems is challenging because of the necessity to deliver high power within very limited space. However, not all patients need full support, as many patients have residual muscle function that can be applied for locomotion. This work introduces a microprocessor-controlled leg (hip-knee-ankle-foot) orthosis (mpLeg) with energy recuperation capabilities at the hip joint. The system redistributes motion energy generated by the patient during walking. In stance phase of walking, energy is stored in an elastic element at the hip joint. This energy can be released by computer control later in the gait phase, to support swing phase motion. This work aims at investigating the influence of the elastic element in the orthotic hip joint on a patient's motion. Experiments conducted with a patient suffering from incomplete paraplegia demonstrated that the motion pattern during walking improved with activated energy recuperation. This observation was made over a wide range of system parameters. The patient used the energy recuperation capabilities of the mpLeg with up to 4.1 J recuperated energy per step, which resulted in a more natural swing phase motion during walking. Therefore energy recuperation at the hip joint is a feasible technology for future supportive devices.

I. INTRODUCTION

Robotic systems are gaining importance for restoration of mobility in patients suffering from lower limb paralysis. According to the National SCI Statistical Center in the year 2017 approx. 358,000 people in the United States live with the consequences of SCI, with an incidence of 17,700 [1]. The majority of the injuries (67.6%) are neurologically incomplete, which means there is still residual neural function present. A significant fraction (20.4%) of the cases suffers from incomplete paraplegia. In the past few years

This work was financed by Ottobock Healthcare Products GmbH, with support of the Austrian Research Promotion Agency (FFG, program "Forschungspartnerschaften", project No. 855585).

Roland Auberger is with the Sensory-Motor, Systems (SMS) Lab, Institute of Robotics and Intelligent Systems (IRIS), Department of Health Sciences and Technology (D-HEST), ETH Zurich, Switzerland and with Ottobock Healthcare Products GmbH, Vienna, Austria (e-mail: Roland.Auberger@ottobock.com)

Robert Riener is with the Sensory-Motor, Systems (SMS) Lab, Institute of Robotics and Intelligent Systems (IRIS), Department of Health Sciences and Technology (D-HEST), ETH Zurich, Switzerland and with the Rehabilitation Group, Spinal Cord Injury Center, Balgrist University Hospital, Medical Faculty, University of Zurich, Switzerland (e-mail: robert.riener@hest.ethz.ch)

Michael Friedrich Russold is with Ottobock Healthcare Products GmbH, Vienna, Austria (e-mail: Michael.Russold@ottobock.com)

Hans Dietl is with Ottobock SE & CO. KGAA, Duderstadt, Germany (e-mail: Hans.Dietl@ottobock.com)

numerous exoskeletons have been developed [2]–[4]. Some of them, like the Ekso GT (Ekso Bionics, Richmond, CA, USA), the ReWalk Personal 6.0 (ReWalk Robotics, Yokneam, Israel) and Indego Personal (Parker Hannifin, Cleveland, OH, USA) are commercially available and have opened up new possibilities in gait therapy. Several research groups are investigating the feasibility of textile exosuits [5]–[7], to provide powered support for people with muscle weaknesses. Powered exoskeletons incorporate batteries and motors to provide power for locomotion. As the actuator bandwidth requirements are high, elastic elements are used in series or in parallel [8] to the motor to decrease the required peak electrical power. Despite large improvements in size and weight, powered exoskeletons are still complex to use, bulky, noisy, and only allow rather slow walking speeds. The C-Brace (Ottobock, Duderstadt, Germany) is a purely passive microprocessor-controlled knee orthotic device [9], designed to support the patient during activities of daily life. It provides high functionality for patients with lower limb paresis or paralysis [10]. However, this system requires a significant amount of residual muscle function at the hip. A large group of patients has functional requirements to a supportive device that are unsatisfied with presently available technology. The residual muscle function of these patients is too good to justify a fully powered exoskeleton, yet insufficient for a purely passive system. Nevertheless, their remaining function can and should be used for locomotion, to prevent inactivity related comorbidities like muscle or bone atrophy. A supportive device based on microprocessor controlled hydraulic actuators is proposed to address the physical deficits of this underserved patient group. Using a custom designed series elastic hydraulic actuator (SEHA) [11], that can store and dissipate energy at the hip joint, the device can redistribute the energy that comes from the user's residual muscle function to facilitate functional gait. Series elastic hydraulic actuators have been used in robotic applications for years [12], [13], mainly because of their advantageous force control characteristics. As the proposed system is intended to support the patient in daily life, this work focuses on the most important locomotion task in daily life: level walking. Biomechanical analysis shows a great deal of eccentric muscle activity in the stance phase of level walking, which means that the muscle-tendon system stores or dissipates kinetic energy in this gait-phase [14]–[17]. To exploit this, a passive exoskeletal device with a SEHA at the hip joint was designed. This work aims at determining the required elastic properties of the SEHA to deliver maximum support. An optimization method was developed and evaluated in a case study with a patient suffering from incomplete paraplegia.

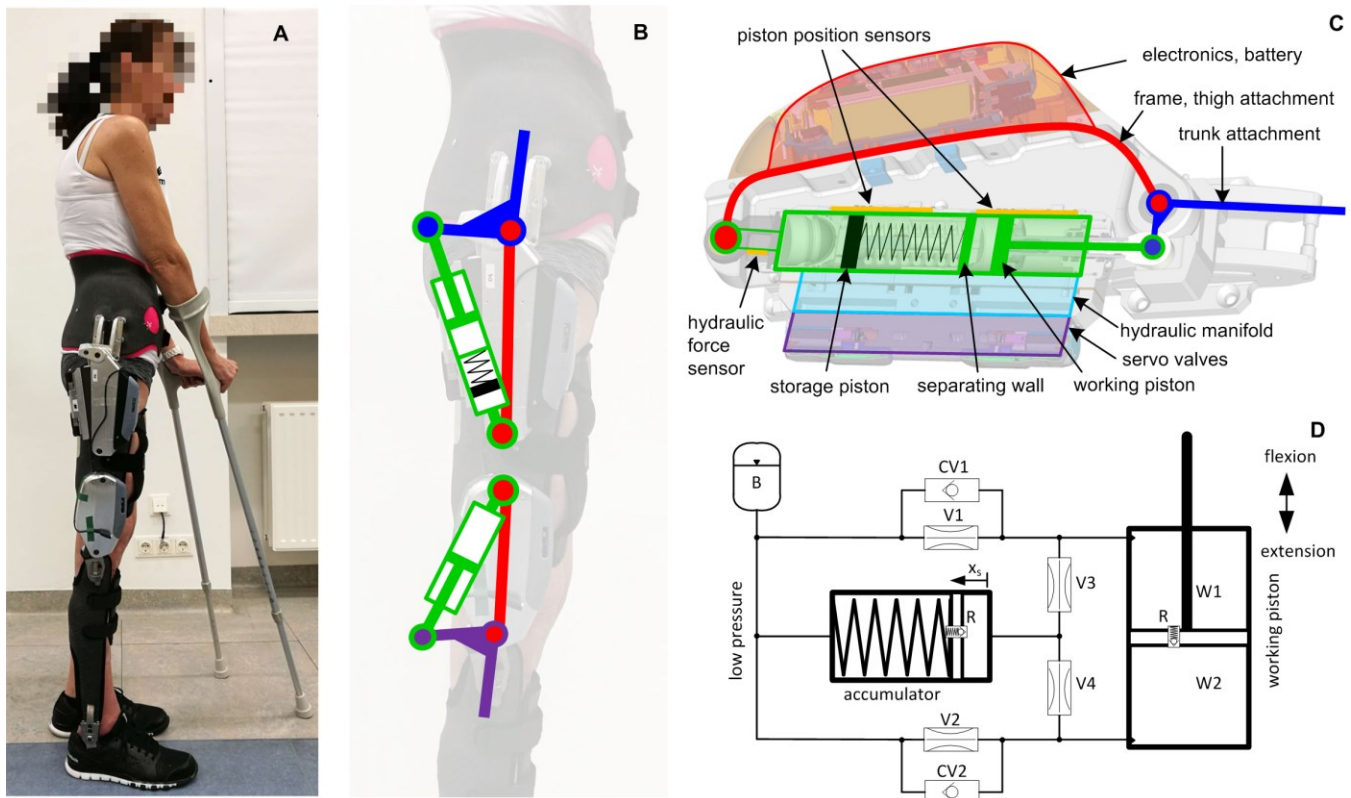


Fig. 1. mpLeg system overview. (A) test subject wearing the system, (B) schematic of lever mechanisms for hip- and knee joint. Blue lines symbolize trunk attachment and lever arm, purple lines shank attachment and lever arm, green lines hydraulic units and red lines thigh attachment. Circles symbolize rotational joints. (C) Cross section and system design layout of hip joint unit, (D) schematic of hydraulic circuitry of the actuator used in the hip joint unit. W... working volumes, V... servo valves, CV... check valves, R... relief valves, B... balancing volume

II. MATERIALS

A prototype of a microprocessor-controlled hip-knee-ankle-foot orthosis (mpLeg) was designed and tested with a single patient.

A. Brace System Design

The hip joint plays a major role for functional mobility support, as it stabilizes the trunk during stance phase and controls thigh motion during swing phase [14]. To support this, an actuator with energy storing capabilities (SEHA) was integrated into the orthosis design. The device stores potential energy via an elastic spring during hip extension in stance phase and uses it to support hip flexion during swing phase (SWP) of gait. To minimize weight the knee and ankle joints are passive, with a microprocessor-controlled damper at the knee joint. The brace system used in the experiments is shown in Fig. 1A. Besides the mechatronic components for hip and knee joint, the mpLeg comprises custom-made components that interface with the body of the patient (trunk-, thigh-, shank-, and foot section). These parts are made of carbon fiber reinforced epoxy, based on a plaster impression model of the patient's anatomy. At the ankle a standard component for a unilateral ankle joint (17LA3=T-16, Ottobock, Duderstadt, Germany) was used on the lateral

side. A microprocessor controlled knee joint unit was mounted at the lateral side. For knee joint details please refer to [9]. At the medial side of the knee, a standard modular knee joint (17B26=L16, Ottobock, Duderstadt, Germany) was used. The trunk section was connected to the thigh section with the microprocessor controlled hip joint incorporating a SEHA. Hip- and knee joint are fully autonomous functional units, each of them with integrated microprocessor-controlled hydraulics, sensors and control circuitries. Each joint contains sensors to measure joint angle, hydraulic force, valve position and oil temperature, an inertial measurement unit (IMU) with 3 accelerometers and 3 gyroscopes, an input for an external trigger signal, a dual mode Bluetooth module for data exchange, and a Li-Ion battery. The hip joint has an additional sensor for the position of the storage piston, which is used to estimate the amount of energy stored. A fully charged battery provides more than seven hours of power autonomy.

B. Hip actuation technology

The key element of the microprocessor controlled hip joint is the SEHA, which is a linear hydraulic actuator with two pistons, as shown in Fig. 1C. The "working piston" is connected to the piston rod and, therefore, creates the interface between the mechanical and the hydraulic system. The "storage piston" lies in a separate chamber and is

connected to a precompressed compression spring that accumulates and stores potential energy. Therefore, it is called the accumulator spring. The parameters (stiffness c and precompression force F_0) of the accumulator spring are essential for the system performance; therefore, this work aims to optimize these parameters. As the SEHA incorporates four servo valves and two check valves in the hydraulic circuitry (cf. Fig. 1D), it has various modes of operation. It can dissipate, store and release energy in any direction of motion. Relief valves limit the maximum actuation force to prevent the mechanical structure from damage in case of overpressure.

C. Joint Kinematics and Properties

As shown in Fig. 1B, linear hydraulic units are used to control knee and hip joints by means of lever mechanisms. These mechanisms transform the linear motion of the hydraulic actuators to the rotational motion of the respective joint. The design of the mechanisms leads to a nonlinear relationship between joint angle and joint torque at a given hydraulic force. Knee and hip joint kinematics were designed to provide functional support in level walking and activities of daily life. Therefore, the lever arm geometry of both joints was chosen to provide an angle dependent torque as shown in Fig. 2. The unique property of the hip joint actuator is its ability to store energy in a spring and release it at any desired position. With this key functionality, the system can store energy in stance phase, and release it at the optimal time determined by the control unit to support swing phase motion. Depending on the parameters of the accumulator spring and the joint kinematics, the energy return of the actuator has typical characteristics as shown in Fig. 2. As the storage piston has only 16 mm stroke (the working piston has 30 mm), only a subset of the range of motion can be supported by the accumulator spring.

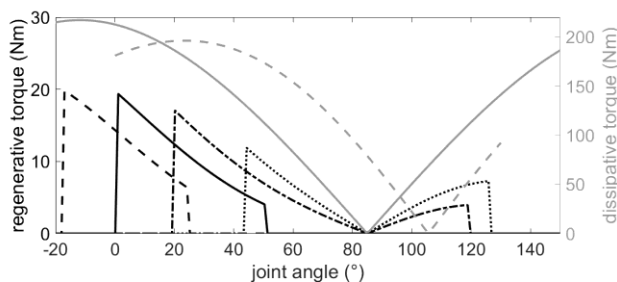


Fig. 2. Torque characteristics of the joints. Hip and knee angle are defined as zero (0°) at quiet standing position, with positive values for flexion movements. Grey, right axis: angle dependent dissipative joint torque at maximum hydraulic force. Solid line: hip joint, dashed line knee joint. Black, left axis: theoretical actuator moment if the spring is released from full compression to create flexion moment, at different angular positions. Spring characteristics: $c = 30500$ N/m, $F_0 = 320$ N. Solid line: spring released at “neutral standing position” (0°), dashed, dash-dotted and dotted lines represent the characteristics if spring is released at various hip flexion and extension angles. Note that the valves must be switched at 85° (hip) and 105° (knee), where the piston motion reverses due to the kinematics to provide flexion moment beyond that point.

The range of support depends on the initial angle of energy return. It is sufficient to support level walking [14]. Due to the kinematics, the motion of the working piston reverses at 85° hip joint and 105° knee joint angle. This allows for relaxed sitting without loads being imposed by the orthosis. The actuator has no effect at this point, because it has no effective lever arm.

The properties of the accumulator spring define the amount of energy stored. With $x_s = 0$ for the storage piston position if no energy is stored, and assuming a linear spring, the amount of energy stored (E_{store}) in the SEHA can be evaluated by:

$$E_{store} = F_0 * x_s + c * \frac{x_s^2}{2} \quad (1)$$

As the storage piston deflection x_s is the only parameter that varies, the storage piston position sensor can be used to estimate the stored energy. Maximum storage capacity is defined by the maximum deflection of the storage piston $x_{s,max} = 16$ mm.

D. Joint Control

Hip and knee joint are controlled individually by state machines on the local microcontroller with an update rate of 100 Hz. As human force control bandwidth is in the order of 20 to 30 Hz [18], the control cycle frequency of 100 Hz is assumed to be perceived as real time control. The Bluetooth link to an external PC is used only for data acquisition and to set patient specific control parameters. Knee joint control is based on the “default stance” principle, which means that the system is always in a safe stance phase (STP) mode, unless sensor information implies that swing phase (SWP) should be initiated. For details on knee joint control please refer to [9]. Only a simple control paradigm for the hip joint was implemented during the experiments. During walking the hip actuator behaved like a nonlinear rotational spring (cf. Fig. 2) with software adjustable neutral position and timed energy release.

III. METHODS

To minimize the influence on the patient's movement during energy storage, the intrinsic hip joint behavior (defined by spring parameters stiffness c and precompression force F_0) should match the force profile of natural motion in the phase of gait where the hip muscles mainly dissipate energy. To achieve that, iterations of simulations and patient tests were pursued: Data obtained in an experiment was fed into an offline optimization algorithm to determine the optimal spring parameters for the next experiment, based on the actual motion pattern of the patient. Between the experiments the spring was exchanged, to achieve properties matching the recent optimization result. It was assumed, that with this method optimization results will converge to an optimum for the respective patient.

A. Hip Joint Parameter Optimization

Hip motion data was fed into a mathematical model of the hip joint, to calculate the expected force profile and corresponding hydraulic pressure based on the patient data. An exhaustive search optimization (60,095 steps) was performed, with the goal to minimize the squared error between the hydraulic pressure generated by the accumulator spring acting on the piston surface area (A_{piston}) and the simulated hydraulic pressure generated by reference motion data (p_{ref}) over a step cycle (SC). Thus, the cost function was:

$$C = \sum_{SC=0\%}^{SC=100\%} \left(\frac{F_0 + c * x_s}{A_{piston}} - p_{ref} \right)^2 \quad (2)$$

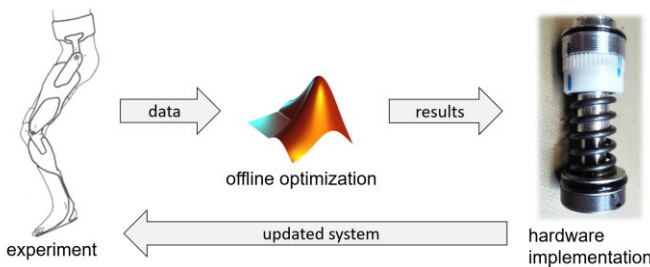


Fig. 3. Optimization process to determine spring parameters.

In addition to determining the optimum ($C = \text{minimum}$) there was also interest in other “good” parameter combinations, where the results for the cost function differ less than 10% from the optimum ($C < \text{min}(C) * 1.1$).

B. Walking Experiments

Walking experiments with one female subject (age 52, height 181 cm, weight 54 kg) suffering from unilateral paralysis of the right leg due to a slipped disc at level Th7-8 were performed. Residual muscle function was assessed at the beginning of the study by a manual muscle test using the Janda scale [19], which quantifies muscle function with scores from 0 (no function) to 5 (normal function). Scores for the affected (right) leg were: Hip ab/adduction: 3/3- Hip flexion/extension: 4/3 Knee flexion/extension 2/5 Foot dorsi/plantarflexion: 3/4, spasticity in M. Gastrocnemius. On the left leg all muscles had normal function. In her everyday life the patient uses a wheelchair, a KAFO and two crutches. The experiments were part of a clinical pilot study, which was conducted at the motion analysis lab of Orthopädisches Spital Speising, Vienna, and at Ottobock Healthcare Products GmbH, Vienna. The study protocol was approved by the ethics committee of the city of Vienna (EK 16-127-0716), and the patient provided informed consent. The patient walked using the system with different spring parameter configurations. The neutral position of the spring and the timing of energy release were adjusted in each setup according to the patient’s preferences. The patient had the possibility to try out the different system configurations in

separate sessions a few days prior to the actual gait analysis. These sessions were used to adjust the brace and for acclimatization, to get consistent results. Additional measurements were performed to verify the functionality of the system and to identify the general effect of the elastic hip support. In the “Knee only” configuration the hip joint was not mounted to the brace. During the “Hip transparent” experiment the hip joint was mounted to the brace, but all valves were opened to minimize the forces imposed by the hydraulics. This measurement was performed to identify the influence of weight and the passive restrictions of the hip joint. In the “setup” experiments elastic hip joint support was activated. Four measurement sessions with different hip joint setups were performed. Results were fed back to the optimization to determine refined spring parameters. Data was collected from the internal joint sensors and with a motion capture system. The elastic hip joint properties (defined by the accumulator spring) were varied between the experiments. Patient data was collected over a multitude of steps. For further analysis steps were automatically identified in the data and normalized to a gait cycle starting from heel strike. As only steps where the patient was walking straight with constant speed were taken into account, the number of analyzed steps varied between the experiments.

IV. RESULTS

The patient was able to walk with the device in all system configurations, using crutches as walking aids. Patient data was collected over a multitude of steps. For further analysis steps were automatically identified in the data and normalized to a gait cycle starting from heel strike.

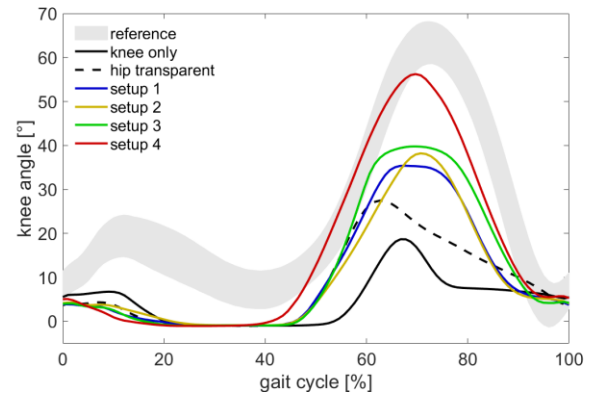


Fig. 4. Measured knee angle (knee joint sensor information) in different patient experiments. Colored lines illustrate averaged data (over several steps) with hip activated in various system setups. Black dashed line: hip joint set to minimum resistance “transparent” mode (18 steps), black solid line: knee support only (71 steps), shaded area: reference data of healthy subjects [17].

A. Device Functionality

The knee angle was the only measurement available in all system configurations (even without hip joint). As the knee joint is in the middle of the kinematic chain of the leg, knee

motion was chosen to judge the general functionality of the device. Fig. 4 illustrates that, for all system setups with activated hip support, knee motion is closer to the motion of healthy subjects compared to configurations without hip support. In the configuration with the softest spring (setup 4), knee motion was closest to the natural motion pattern. The increased maximum knee angle during swing phase led to increased toe clearance, which might reduce the risk of stumbling.

B. Optimization based on reference data

To define the spring parameters for the first experiment, reference data from healthy subjects [20] were used. For a patient weight of 100 kg (maximum patient weight in the system specification) the optimization suggested $c = 32,000$ N/m and $F_0 = 220$ N as optimum spring parameters. There was a large field of “good” parameters with less than 10% deviation from the optimum, which gives some design freedom (cf. Fig. 5). Based on this result and the geometric restrictions of the design, a spring that was available in stock (Febrotec, Germany) with normative parameters $c = 30,542$ N/m and $F_0 = 320$ N was chosen for the first experimental setup (setup 1).

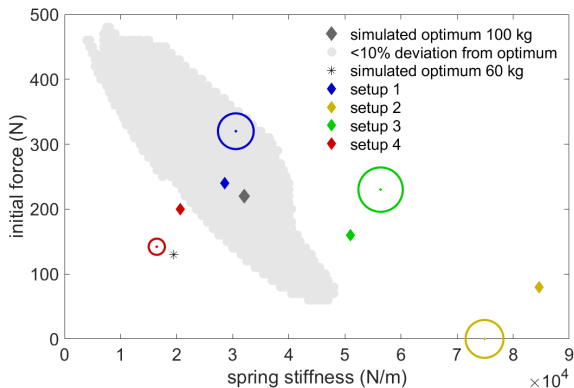


Fig. 5. Results of optimization for accumulator spring parameters and patient experiments. Black and grey correspond to simulations based on reference data from healthy subjects [20], colors correspond to patient experiments with various setups. Dots and circles visualize the experimental setups. The size of the circles corresponds to the maximum stored energy for the respective setup. Diamonds and stars show optimization results based on experimental data (colors) or reference data (grey, black).

For comparison another simulation with reference data was performed, to determine the optimum values for a 60 kg person (which is close to the test patient). Optimum parameters for this case would be $c = 19,500$ N/m and $F_0 = 130$ N, as indicated by the star in Fig. 5. To keep the figure clear the region with <10% deviation from optimum is not shown for this case.

C. Iterative Optimization of Hip Joint Parameters

The measurements (hip angle and hydraulic pressure in the hip joint) of the walking experiments with the hip joint were fed into the offline optimization. Table I and Fig. 5 sum up the system parameters and results for the respective system

setups. According to the prediction based on reference data (cf. section IV.B), it was expected that the optimization would suggest a much softer spring after the first experiment, because the test subject only weighted 54 kg. However, the optimization result was close to the actual spring parameters, especially regarding spring stiffness. As we investigated a wide range of system configurations to test the validity of our method, a totally different set of parameters with a very stiff spring and no precompression was implemented in the second experiment (setup 2). Again, the offline optimization results were close to the actual system parameters of setup 2. Similar observations were made after the 3rd and 4th experiment where an even wider range of parameters was investigated.

D. Energy exchange

The storage capacity used by the patient was defined by the patient’s range of motion. This was influenced by the reaction forces of the system, which the patient had to overcome. It can be seen in TABLE I that, for setups with stiff springs, storage piston travel was reduced. However, despite the differences in spring parameters, the amount of energy stored was in a similar range (3.3 J to 4.1 J per step) for the first three setups. For the last setup (with the softest spring) it was significantly lower (1.5 J).

TABLE I
EXPERIMENT PARAMETERS AND OPTIMIZATION RESULTS

		setup 1	setup 2	setup 3	setup 4
system parameters	c (N/m)	30,542	74,900	56,363	16,446
	F_0 (N)	320	0	230	142
analyzed steps		31	56	22	8
optimization result	c (N/m)	28,600	84,600	51,000	20,600
	F_0 (N)	240	80	160	200
energy stored (J)		3.3	3.5	4.1	1.5
storage piston travel (mm)		10.4	9.2	9.2	10.2

V. DISCUSSION

The approach to iteratively optimize system parameters based on results of measurements with the patient did not lead to the expected result. After the experiments the optimization results were always in a similar range as actual system parameters in the respective experiment. This indicates that the proposed method is an identification method for the system properties, rather than a method to optimize the spring parameters for the patient. One possible explanation is that the patient adapted to the system properties, intuitively trying to optimize motion in order to minimize metabolic effort. The changes in storage piston travel indicate that hip motion was altered as a reaction to changes in the compliance provided by the supportive system. Interestingly, the amount of stored energy in the system was relatively constant (between 3.3 J and 4.1 J per

step) over a wide range of spring parameters. It is assumed that this is the maximum amount of energy that is efficient for the patient to invest into energy storage and return during level walking, in order to minimize overall energy consumption. For stiff springs range of motion and storage piston travel were lower. One possible cause for this reduction in range of motion is the reaction force of the spring. However, also for soft springs, the maximum piston travel (16 mm) was not fully used. The optimization based on reference data from healthy subjects predicted a wide range of “good” parameter combinations with less than 10% deviation from the optimum. This could also be observed in the experiments, as the amount of energy recuperated was similar over a wide range of parameters. “Setup 4”, which was closest to the simulated optimum setup for the weight range of the patient, resulted in the most natural motion pattern, although the amount of energy stored was low compared to the other setups. This can be explained with the course and timing of force development, which were closest to natural for that setup. These results indicate that a prediction based on reference data from healthy subjects is an effective way to determine system parameters.

Although the motion of the patient observed in this study improved with the hip joint support, she had enough hip control to walk without hip support as well. This might be a reason for the observed adaptation to different system setups, especially because the neutral position of the spring was chosen according to the patient’s preferences. Additionally the patient had the chance to train with the respective device prior to all experiments, which provided the opportunity to adapt the motion pattern accordingly. This might not apply to patients with less residual muscle function who may profit from such a system even more. Consequently further experiments, with more severely affected patients, are necessary. These experiments could include measurements (e.g. electromyography) to assess residual muscle activity. Another field for future research would be the application of energy recuperation at the knee or ankle joint.

VI. CONCLUSION

The proposed orthosis with an elastically supporting hip joint improved the patient’s motion during walking over a wide range of system parameters, demonstrating that energy recuperation at the hip can be a suitable method to improve the gait of people with lower limb paralysis. Simulations based on motion data from healthy subjects appear to be an effective method for determining appropriate, beneficial system parameters for a patient.

ACKNOWLEDGMENT

The authors would like to thank the test subject for participating in the study. Furthermore, we would like to acknowledge orthotic team members Kerstin Hofmann, Sonja Wagner and Beate Kiene for manufacturing the custom brace, and physical therapist Monique Bongers for

their project contributions. Dr. Alexander Krebs and Dr. Andreas Kranzl supported the project from the clinical side.

REFERENCES

- [1] National Spinal Cord Injury Statistical Center, “Spinal Cord Injury Facts and Figures at a Glance 2018,” University of Alabama at Birmingham, Birmingham, AL, 2018 SCI Datasheet.
- [2] B. Chen *et al.*, “Recent developments and challenges of lower extremity exoskeletons,” *J. Orthop. Transl.*, vol. 5, pp. 26–37, Apr. 2016.
- [3] L. E. Miller, A. K. Zimmermann, and W. G. Herbert, “Clinical effectiveness and safety of powered exoskeleton-assisted walking in patients with spinal cord injury: systematic review with meta-analysis,” *Med. Devices Auckl. NZ*, vol. 9, pp. 455–466, 2016.
- [4] A. J. Young and D. P. Ferris, “State of the Art and Future Directions for Lower Limb Robotic Exoskeletons,” *IEEE Trans. Neural Syst. Rehabil. Eng.*, vol. 25, no. 2, pp. 171–182, Feb. 2017.
- [5] J. Bae *et al.*, “A soft exosuit for patients with stroke: Feasibility study with a mobile off-board actuation unit,” in *2015 IEEE International Conference on Rehabilitation Robotics (ICORR)*, 2015, pp. 131–138.
- [6] V. Bartenbach, K. Schmidt, M. Naef, D. Wyss, and R. Riener, “Concept of a soft exosuit for the support of leg function in rehabilitation,” in *2015 IEEE International Conference on Rehabilitation Robotics (ICORR)*, 2015, pp. 125–130.
- [7] K. Schmidt *et al.*, “The Myosuit: Bi-articular Anti-gravity Exosuit That Reduces Hip Extensor Activity in Sitting Transfers,” *Front. Neurobotics*, vol. 11, Oct. 2017.
- [8] S. Jung, C. Kim, J. Park, D. Yu, J. Park, and J. Choi, “A wearable robotic orthosis with a spring-assist actuator,” in *2016 38th Annual International Conference of the IEEE Engineering in Medicine and Biology Society (EMBC)*, 2016, pp. 5051–5054.
- [9] R. Auberger, C. Breuer-Ruesch, F. Fuchs, N. Wismer, and R. Riener, “Smart Passive Exoskeleton for Everyday Use with Lower Limb Paralysis: Design and First Results of Knee Joint Kinetics,” in *2018 7th IEEE International Conference on Biomedical Robotics and Biomechanics (Biorob)*, 2018, pp. 1109–1114.
- [10] T. Schmalz, E. Probsting, R. Auberger, and G. Siewert, “A functional comparison of conventional knee–ankle–foot orthoses and a microprocessor-controlled leg orthosis system based on biomechanical parameters,” *Prosthet. Orthot. Int.*, Sep. 2014.
- [11] R. Auberger, H. Sima, and M. Seyr, “Actuator-Damper Unit,” US2018098864 (A1), 12-Apr-2018.
- [12] D. W. Robinson and G. A. Pratt, “Force controllable hydro-elastic actuator,” in *Proceedings 2000 ICRA. Millennium Conference. IEEE International Conference on Robotics and Automation. Symposia Proceedings*, San Francisco, CA, USA, 2000, vol. 2, pp. 1321–1327.
- [13] A. G. L. Junior, R. M. de Andrade, and A. B. Filho, “Linear Serial Elastic Hydraulic Actuator: Digital Prototyping and Force Control,” *IFAC-Pap.*, vol. 48, no. 6, pp. 279–285, 2015.
- [14] J. Perry and J. M. Burnfield, *Gait Analysis: Normal and Pathological Function*, 2 ed. Thorofare, NJ: Slack Inc, 2010.
- [15] D. J. Farris and G. S. Sawicki, “The mechanics and energetics of human walking and running: a joint level perspective,” *J. R. Soc. Interface*, vol. 9, no. 66, pp. 110–118, Jan. 2012.
- [16] M. Kuster, S. Sakurai, and G. A. Wood, “Kinematic and kinetic comparison of downhill and level walking,” *Clin. Biomech. Bristol Avon*, vol. 10, no. 2, pp. 79–84, Mar. 1995.
- [17] G. Bovi, M. Rabuffetti, P. Mazzoleni, and M. Ferrarin, “A multiple-task gait analysis approach: Kinematic, kinetic and EMG reference data for healthy young and adult subjects,” *Gait Posture*, vol. 33, no. 1, pp. 6–13, Jan. 2011.
- [18] H. Z. Tan, B. Eberman, M. A. Srinivasan, and B. Cheng, “Human factors for the design of force-reflecting haptic interfaces,” *American Society of Mechanical Engineers, Dynamic Systems and Control Division (Publication) DSC*, 01-Dec-1994.
- [19] V. Janda, *Muscle Function Testing*. Elsevier, 2013.
- [20] D. Waldmann, “Biomechanik der Gehens auf verschiedenen Neigungen- eine kinetische, kinematische und elektromyographische Untersuchung.” Magisterarbeit, Georg-August-Universität, Göttingen, 2006.